

Electrode Polarization for Nylon 1010 with Dielectric Relaxation Spectroscopy

Hongbo Lu,¹ Xingyuan Zhang,¹ Bo He,¹ Hui Zhang²

¹Department of Polymer Science and Engineering, University of Science and Technology of China, Hefei 230026, People's Republic of China

²Department of Applied Physics, Anhui University, Hefei 230039, People's Republic of China

Received 3 November 2005; accepted 31 December 2005

DOI 10.1002/app.23987

Published online in Wiley InterScience (www.interscience.wiley.com).

ABSTRACT: Electrode polarization arising from charge carriers accumulating at the interface between an electrode and nylon 1010 was investigated with dielectric relaxation spectroscopy. In the frequency spectra of nylon 1010, the dielectric permittivity showed high values in the region of low frequencies and high temperatures. With the Havriliak–Negami function used to fit the experimental spectra, the result revealed that the high values originated from electrode polarization and direct-current conductivity. For electrode polarization, the dielectric strength, independent of the temperature, was about 1150, and the temperature dependence of the relaxation time followed the Vogel–Tammann–Fulcher equation. Fitting with the Vogel–Tam-

mann–Fulcher equation, the parameters $\tau_0 = 1.33 \times 10^{-10}$ s and $T_0 = 303.2$ K were proposed (where τ_0 is the relaxation time at a very high temperature and T_0 is the temperature at which the relaxation time becomes extremely large), and they suggested that the motion of the polymeric chains was one of the factors leading to charge-carrier transport at temperatures higher than the glass-transition temperature. © 2006 Wiley Periodicals, Inc. *J Appl Polym Sci* 102: 3590–3596, 2006

Key words: charge transport; dielectric properties; nylon; relaxation

INTRODUCTION

Nylon 1010, which has a molecular structure analogous to that of nylon 66, is one of the most important polyamide engineering plastics and is widely used in industry.^{1–3} Moreover, like other polyamides, nylon 1010 is a typical semicrystalline polymer with different microstructures under various thermal histories.⁴ The investigation of the electrical and dielectric properties of nylon 1010 is important from both fundamental and technological points of view.

Dielectric relaxation measurements have been widely employed to investigate the nature of the molecular motion of nylons.^{5–7} Relatively less attention has been paid to the electrical and dielectric behaviors of nylons in dielectric relaxation spectra at high temperatures, especially those higher than the glass-transition temperature (T_g). Several dielectric studies of nylons have revealed the existence of low-frequency/high-temperature polarization in addition to the primary α relaxation and the secondary β and γ relaxations. The low-frequency/high-temperature polarization has been attributed to the motion of am-

ide-group hydrogen involved in intermolecular hydrogen bonds.⁸ Steeman and Maurer⁹ observed that the ionic conductivity in nylon 46 dominates at temperatures higher than T_g and gives rise to strong Maxwell–Wagner–Sillars (MWS) polarization. Pathmanathan and Johari¹⁰ analyzed the results of dielectric measurements for nylon 12 in the temperature range of 27–177°C by means of dielectric permittivity, alternating-current conductivity (σ_{ac}), and electric modulus formalism, and they concluded that high dielectric permittivity at a low-frequency region was contributed by conductivity relaxation. In the low-frequency region of dielectric relaxation spectra of RbSn₂F₅, Bi₂Ti₄O₁₁, poly(ethylene terephthalate) (PET), poly(methyl methacrylate), and other materials, an increase in the dielectric permittivity has been systematically observed at temperatures well above T_g .^{11–15} This phenomenon is usually attributed to the contribution of σ_{ac} from different electrical mechanisms, such as the free charge, ionic conductivity, hopping conductivity, blocking charge in the electrode, and interfacial effects depending on the material measured and on the type of electrode used.^{11,15,16}

To investigate further the electric and dielectric behavior and polarization mechanism for nylon 1010, we measured the dielectric relaxation spectra in the frequency range of 100 Hz to 5 MHz. The research point was the electric behavior in the region of low frequencies and high temperatures. The results

Correspondence to: X. Zhang (zxym@ustc.edu.cn).

Contract grant sponsor: National Natural Science Foundation of China; contract grant number: 50273035.

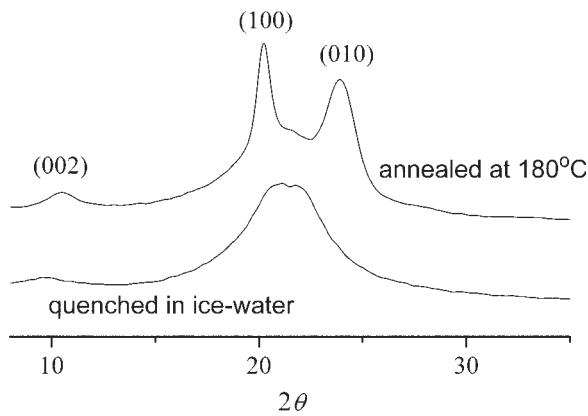


Figure 1 WAXD curves of nylon 1010.

revealed that the high values of the dielectric permittivity were due to the direct-current conductivity (σ_{dc}) and electrode polarization. Much attention was paid to the electrode polarization. Through the fitting of the dielectric relaxation data, the relaxation strength and relaxation time for electrode polarization were proposed.

EXPERIMENTAL

A granular sample of nylon 1010 was obtained from Yixing Chemicals (Yixing, China). A quenched film about 0.15 mm thick was prepared through the quenching of a melt-pressed film in an ice-water bath. An annealed sample was prepared through the annealing of the quenched sample at 180°C *in vacuo* for 2 h.

Wide-angle X-ray diffraction (WAXD) measurements were carried out on a Philips Dual X'Pert diffractometer (Eindhoven, Netherlands) with Cu K α radiation over the diffraction angle (2θ) range of 8–35°.

The two sides of the annealed sample were coated with a silver electrode 10 mm in diameter for dielectric measurements. The dielectric permittivity was measured with a Hioki 3532 LCR meter (Nagano, Japan) in the frequency range of 100 Hz to 5 MHz.

RESULTS AND DISCUSSION

The crystal structure of nylon 1010 belongs to the triclinic system.³ WAXD is commonly employed for studies of the crystal form, unit cell, degree of crystallinity (X_c) and crystallite dimension of polymer samples under various conditions. WAXD intensity curves for nylon 1010 before and after annealing are displayed in Figure 1. For the annealed sample, three characteristic peaks at 2θ values of 10.5, 20, and 24°, corresponding to the reflection of (002), (100), and (010) planes, can be observed clearly. For the quenched sample, only one wide peak corres-

ponding to an amorphous phase appears at about $2\theta = 21.5^\circ$. According to the intensity curves, X_c of the sample was calculated with the following formula proposed by Huang et al.:¹⁷

$$X_c = \frac{I_{010} + 0.064I_{002} + 0.57I_{100}}{I_{010} + 0.064I_{002} + 0.57I_{100} + 0.504I_a} \times 100\% \quad (1)$$

where I_{hkl} is the area under the diffraction peak and I_a is the area under the peak corresponding to the amorphous phase. The calculated results showed that X_c for the annealed sample was about 47%, whereas that for the quenched one was about 0. In this study, the experimental temperature was never heated above 180°C so that X_c of the annealed sample could be kept practically constant during the measurement.

The temperature dependence of the real part (ϵ') and imaginary (ϵ'') part of the dielectric permittivity ($\epsilon^* = \epsilon' - i\epsilon''$, i is the square root of -1) of annealed samples at five different frequencies is shown in

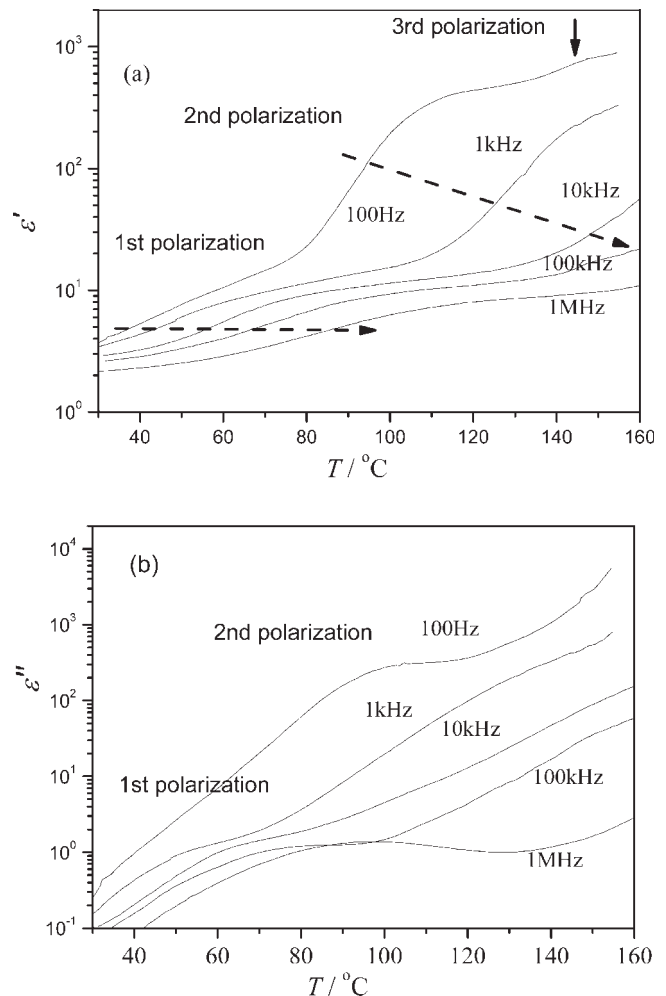


Figure 2 Temperature (T) dependence of ϵ' and ϵ'' for nylon 1010 at five different frequencies.

Figure 2. Three polarization processes are clearly visible. The first process can be observed in the low-temperature region as a step in Figure 2(a). With the frequency increasing from 100 Hz to 1 MHz, the step shifts from 40 to about 90°C. In isochronal ϵ'' plots, as shown in Figure 2(b), the corresponding dielectric loss maximum (ϵ''_{\max}) can be found from about 50 to 90°C as the frequency varies from 1 kHz to 1 MHz. When the frequency decreases to 100 Hz, ϵ''_{\max} , masked by the high-temperature relaxation and σ_{dc} , cannot be observed clearly. A similar relaxation process in other nylons^{5,9} has been called α relaxation and attributed to the orientation of amide groups in the amorphous regions, which are controlled by the motions of large segments of the molecule. Similar to the first process, the second polarization also appears as a step in Figure 2(a) from 95 to 150°C as the frequency varies from 100 Hz to 10 kHz. When the frequency is larger than 10 kHz, the polarization step shifts to a higher temperature out of the measurement temperature range. The values of ϵ' and ϵ'' of this polarization are much larger than those of the first relaxation process. This polarization process is due to charge carriers accumulating at the interface between the amorphous region and crystalline region; seen in nylon 46 and nylon 66, it is called MWS polarization.⁹ Also as a step, the third polarization process can be found from the curve of 100 Hz in Figure 2(a) at about 145°C, but the corresponding dielectric loss peak is not visible in Figure 2(b) because of the high conductivity. With increasing frequency, the third polarization shifts to a higher temperature and out of the measurement range.

To further study the third polarization, it was necessary to investigate the frequency dependence of the dielectric permittivity in detail at temperatures higher than 100°C. The frequency dependence of ϵ' , ϵ'' , and $\tan \delta$ ($\tan \delta = \epsilon''/\epsilon'$) at several temperatures between 100 and 160°C for nylon 1010 is shown in Figure 3. Only two relaxation processes can be observed. The first process can be seen in the high-frequency region as a step in Figure 3(a). With an increase in the temperature, the step shifts to the frequency region over megahertz, indicating a thermally activated process in the high-frequency region. Comparing Figure 3 with Figure 2, we find that this relaxation corresponds to the α process and can be attributed to the orientation of amide groups in the amorphous region. In isochronal plots of ϵ'' and $\tan \delta$, as shown in Figure 3(b,c), only part of the corresponding broad peak can be found.

Another large relaxation process appears at a relatively low-frequency region in Figure 3. ϵ' and ϵ'' increase rapidly with decreasing frequency and increasing temperature and become higher than 10^3 ; they do not obviously correspond to the bulk dielectric char-

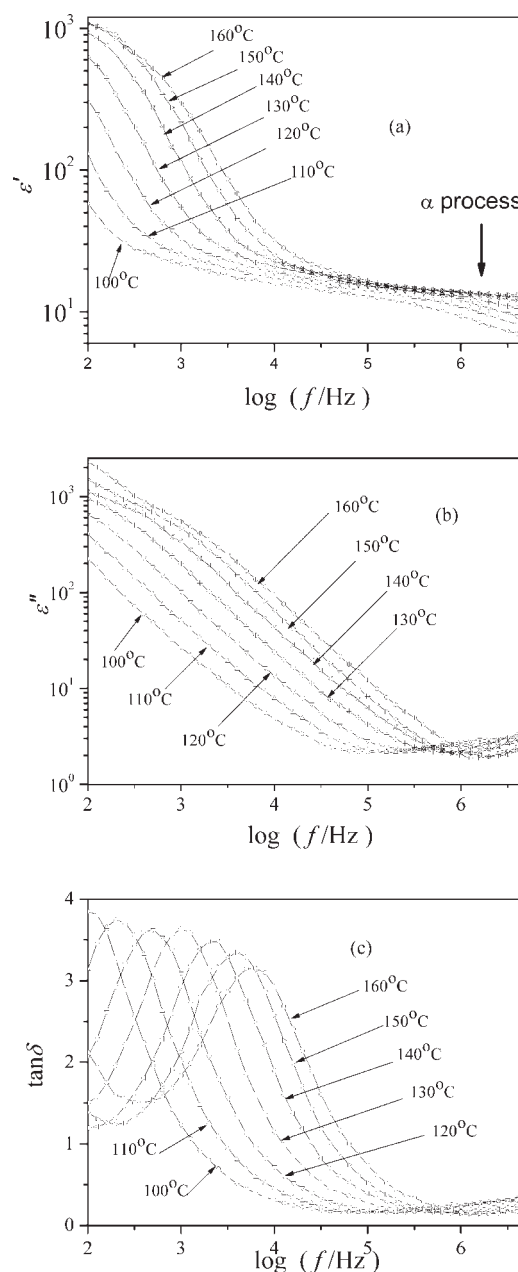


Figure 3 Frequency (f) dependence of ϵ' , ϵ'' , and $\tan \delta$ for nylon 1010.

acteristics of nylon 1010. Corresponding to the relaxation process, $\tan \delta$ shows a typical peak in Figure 3(c). The peak location shifts to a higher frequency and the peak height decreases with increasing temperature. Similar phenomena have been observed for PET and poly(hydroxyethyl acrylate)/water hydrogels.^{13,18} The high ϵ' value was attributed to the charge carriers accumulating at the interface within the sample (interfacial or MWS polarization⁹) and/or at the interfaces between the sample and the electrodes (electrode polarization or space charge polarization^{13,18}). The high ϵ'' value originated from the

direct-current conductivity (σ_{dc}) in addition to these polarizations. Comparing the values shown in Figure 3 in the high-frequency range with those in the low-frequency range, we find that the effect of α relaxation for nylon 1010 in the high-frequency region can be neglected.

For very low frequencies, there is enough time for the charge carriers to move macroscopic distances and to accumulate at the interfaces between the sample and the electrodes before the field changes direction, giving a very high value of ϵ' (electrode polarization). With increasing frequency, there is no enough time for the charge carriers to accumulate at the sample–electrode interfaces; there is time only for the transport of the charge carriers over microscopic and mesoscopic dimensions and their accumulation at the boundaries of conducting species in the material (MWS polarization). At even higher frequencies, the charge carriers cannot follow the changes in the electric field, and only the bulk polarization mechanisms characteristic of the molecular structure (α and β processes) contribute to the electric polarization and thus to ϵ' .^{18,19}

To further elucidate the microscopic mechanisms and accompanying polarization phenomena of the charge-carrier transport, it is necessary to study the dependence of the frequency and temperature for the alternating-current conductivity (σ_{ac}). According to the following equation, σ_{ac} can be obtained easily.¹⁶

$$\sigma_{ac} = \omega \epsilon_0 \epsilon'' \quad (2)$$

where $\omega = 2\pi f$ (f is the frequency) is the angular frequency and $\epsilon_0 = 8.854 \times 10^{-12}$ F/m is the absolute permittivity of free space. Figure 4 shows the frequency dependence of σ_{ac} over a wide range of frequencies for nylon 1010 from 100 to 160°C. σ_{ac} changes drastically with the temperature and fre-

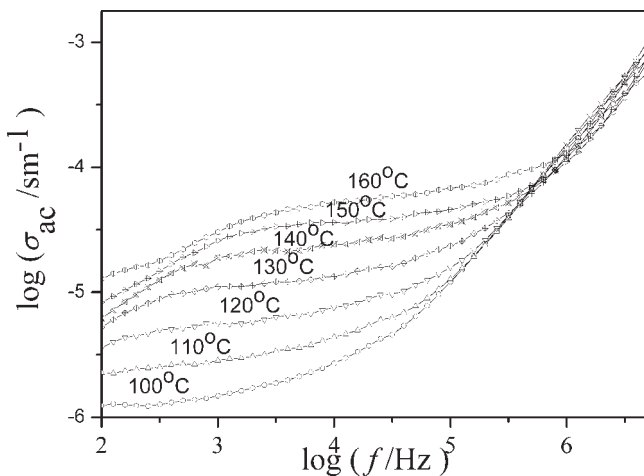


Figure 4 Frequency (f) dependence of σ_{ac} for nylon 1010.

quency. A plateau (a region in which σ_{ac} is frequency-independent) can be observed clearly in the curves. The values corresponding to the plateau are usually identified with σ_{dc} of the material at the respective temperature.²⁰ In the high-frequency region, σ_{ac} exhibits a dispersion increasing rapidly with increasing frequency. The transition region from direct-current conductivity (frequency-independent) to alternating-current conductivity (frequency-dependent) shifts to a higher frequency with an increase in the temperature.

An additional feature, which can be seen in the curves at high temperatures ($> 110^\circ\text{C}$) in Figure 4, is a reduction of σ_{ac} at frequencies below the σ_{dc} region. This drop can be ascribed to the electrode polarization,^{11,13} which has different polarization mechanisms with the dielectric bulk. As the frequency decreases, more and more charge carriers accumulate at the interface between the sample surface and the electrode, and this leads to the drop in σ_{ac} in the low-frequency region. This drop shifts to a higher frequency with increasing temperature. The electrode polarization effect becomes increasingly important at high temperatures, reflecting the enhancement of the mobility of charge carriers.

MWS polarization is due to the accumulation of charge carriers at the interfaces between the amorphous region and crystalline region within nylon 1010, and MWS polarization appears within the σ_{dc} region for the sample as a whole. Comparing Figures 3(a) and 4, we can confirm that electrode polarization rather than MWS polarization should be the origin of high ϵ' values in the region of low frequencies and high temperatures, as the high values of ϵ' appear within the σ_{ac} drop region. Following this consideration, we have attributed the third polarization process in Figure 2, electrode polarization, to charge carriers accumulating at the interfaces between the sample and the electrodes.

The model of Coelho assumes that when an electric field is applied to a sample, the charge carriers move through the sample toward the electrode of opposite sign and finally build up a macrodipole at the interfaces between the sample and the electrodes.¹⁴ Therefore, the frequency dependence of electrode polarization also can be described by the Havriliak–Negami function.²¹ Considering the contribution of σ_{dc} ($-i\sigma_{dc}/\epsilon_0\omega$), the Havriliak–Negami equation can be used to fit the experimental data:^{21,22}

$$\epsilon^* = \epsilon_\infty + \sum_j \frac{(\Delta\epsilon)_j}{[1 + (i\omega\tau_j)^{\alpha_j}]^{\beta_j}} - i \frac{\sigma_{dc}}{\epsilon_0\omega} \quad (3)$$

where ϵ_∞ denotes the dielectric constant in the high-frequency limit; $\Delta\epsilon$ is the dielectric strength; and α_j and β_j are the distribution and skewness parameters of the j polarization process, respectively. In this

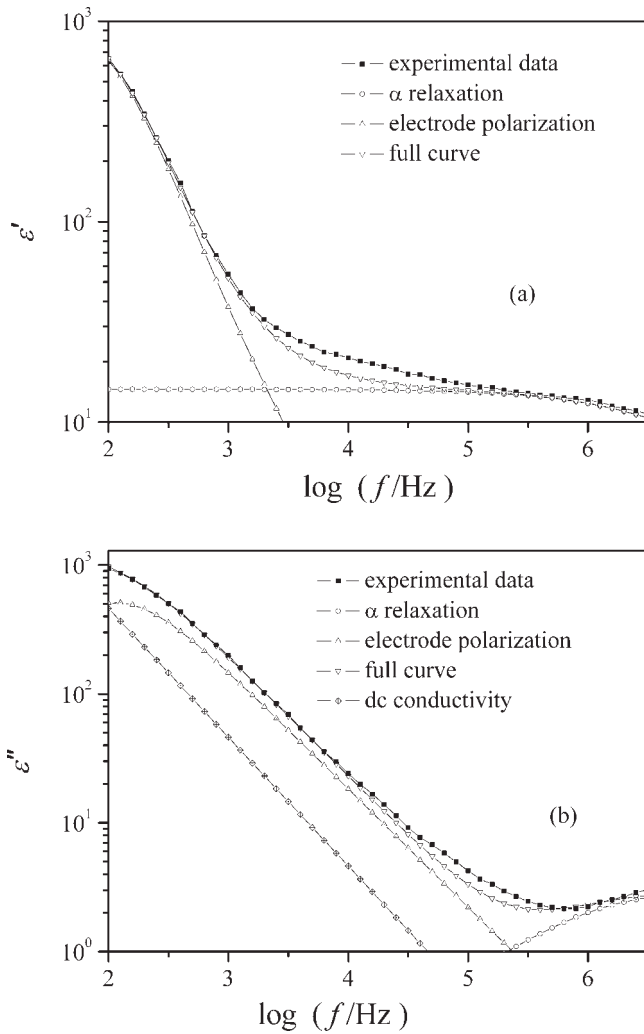


Figure 5 Curve fitting of the experimental ϵ' and ϵ'' values for nylon 1010 measured at 140°C (f = frequency).

article, j ranges from 1 to 2, and the polarization processes include electrode polarization and α polarization. The fitting of the experimental dielectric spectra was carried out with software developed in our laboratory.

The experimental results were fitted to eq. (3) with the constraints $0 \leq \alpha \leq 1$ and $0 \leq \beta \leq 1$. The fitting processes were performed through the multidimensional minimization of relative errors with $\Delta\epsilon$, α , β , τ , ϵ_{∞} , and σ_{dc} as variable parameters. One example of the fitting procedure is plotted in Figure 5. It shows a good agreement between the experimental curve and full curve (sum of the α relaxation, electrode polarization, and σ_{dc}), except for the middle-frequency region. This difference is due to MWS polarization in the middle-frequency region. For electrode polarization, parameter α is 1, and β lies between 0.88 and 0.94. These parameters show that the electrode polarization has some relaxation time distribution. For the α process, α is in the range of

0.49–0.66, and β lies between 0.68 and 0.82. These parameters show that the α process has a wide relaxation time distribution.

The frequency dependence of ϵ'_{elec} , ϵ''_{elec} , and $\tan \delta_{elec}$ for electrode polarization is shown in Figure 6. ϵ'_{elec} and ϵ''_{elec} refer to the electrode polarization contributions to dielectric permittivity. The $\Delta\epsilon$ value of electrode polarization is practically independent of the temperature; this differs from α relaxation. The fitting result gives a $\Delta\epsilon$ value of electrode polarization of approximately 1150, which is much larger

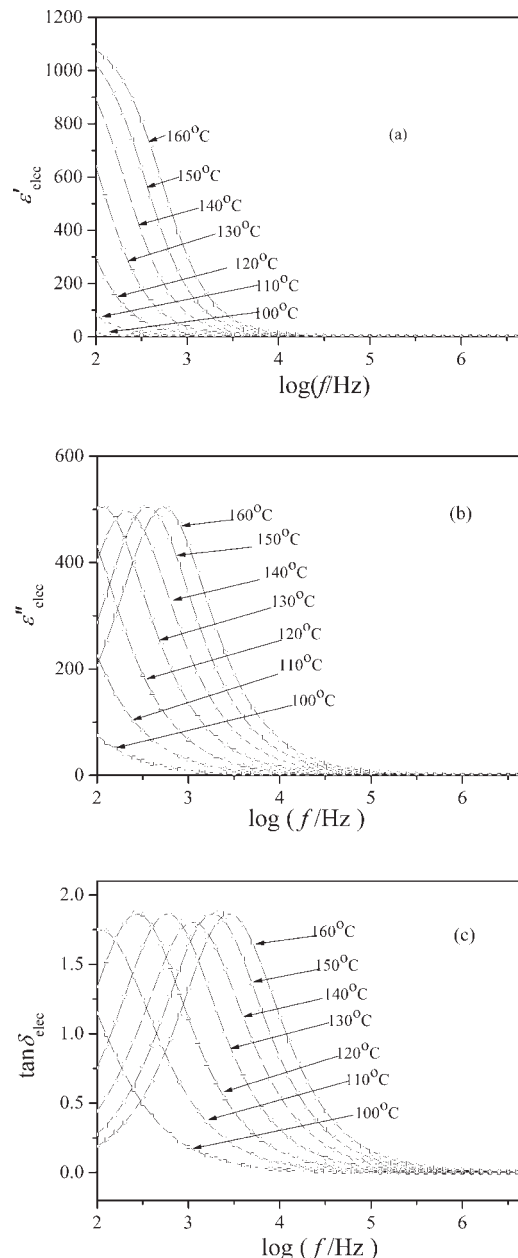


Figure 6 Frequency dependence of ϵ'_{elec} , ϵ''_{elec} , and $\tan \delta_{elec}$ for the electrode polarization of nylon 1010 (f = frequency).

than that of the α relaxation. Such a high $\Delta\epsilon$ value is due to the distinct difference in the conductance of nylon 1010 and the electrodes.

On the basis of the fitting results, the pure loss by electrode polarization can be observed clearly in Figure 6(b). The ϵ''_{elec} peak shifts to a high frequency with increasing temperature, and the maximum ϵ''_{elec} value is about 500. The frequency dependence of $\tan \delta_{\text{elec}} = \epsilon''_{\text{elec}}/(\epsilon'_{\text{elec}} + \epsilon_{\text{com}})$ is shown in Figure 6(c). Here ϵ_{com} is the completely relaxed constant of high-frequency processes, including MWS and the α -relaxation or unrelaxed dielectric constant of electrode polarization.²³ The peak of $\tan \delta_{\text{elec}}$ shifts to a high frequency with increasing temperature, and the magnitude is independent of the temperature. In comparison with Figure 3(c), it is understood that the magnitude of $\tan \delta$ decreases with increasing temperature because $\tan \delta$ consists of σ_{dc} , MWS polarization, and α relaxation, except for the electrode polarization.

According to the frequency of the ϵ'' peak shown in Figure 6(b), the relaxation time for electrode polarization (τ_{elec}) can be obtained. Figure 7 shows a relationship between $\ln \tau_{\text{elec}}$ and the inverse of the temperature. τ_{elec} decreases with increasing temperature, presenting an enhancement of the mobility of charge carriers at high temperatures. For the main relaxation and conductivity relaxation in a polymer, the temperature dependence of τ follows the Vogel–Tammann–Fulcher (VTF) equation:^{23,24}

$$\tau = \tau_0 \exp\left(\frac{B}{T - T_0}\right) \quad (4)$$

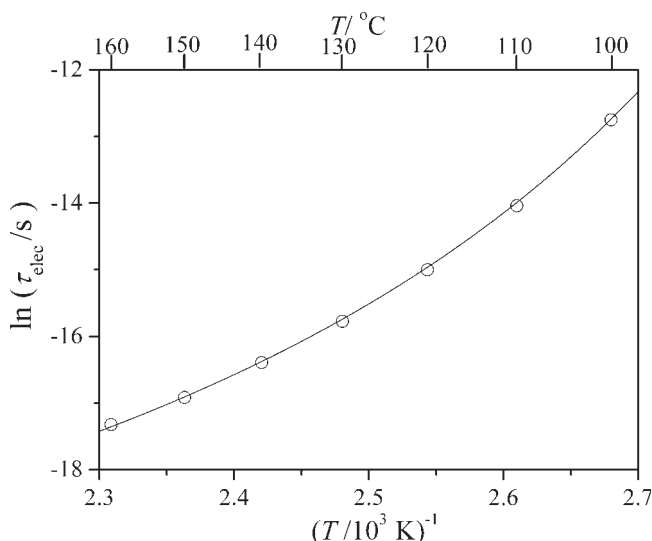


Figure 7 Correlation of τ_{elec} with the temperature (T) for the electrode polarization of nylon 1010. The solid line represents the fitting equation.

where B is a constant, τ_0 is the relaxation time at a very high temperature, and T_0 is the temperature at which the relaxation time becomes extremely large. The VTF equation was originally proposed to describe the scaling behavior of viscosity and was extended to describe the dielectric relaxation time under the assumption that τ is proportional to the viscosity according to the Maxwell model for viscoelasticity. From the curve shape in Figure 7, τ_{elec} seems to be fitted suitably by the VTF equation. When the curve was fitted with eq. (4), the parameters $\tau_0 = 1.33 \times 10^{-10}$ s, $B = 700$ K, and $T_0 = 303.2$ K were determined. Similarly to the temperature dependence of σ_{dc} in a polymer,^{13,20} these results show that the motion of polymeric chains is one of the factors leading to charge-carrier transport at temperatures higher than T_g .

CONCLUSIONS

The influence of electrode polarization on the dielectric relaxation properties of nylon 1010 has been investigated with dielectric relaxation spectroscopy over a wide range frequencies (100 Hz to 5 MHz). The dielectric permittivity shows high values in the region of low frequencies and high temperatures because of σ_{dc} and electrode polarization. The $\Delta\epsilon$ value of electrode polarization is independent of the temperature, and the relaxation time decreases with increasing temperature. The temperature dependence of the relaxation time follows the VTF equation, which shows that the motion of the polymeric chains is one of the factors leading to charge-carrier transport at temperatures higher than T_g .

References

1. Yang, X.; Li, G.; Zhou, E. *Macromol Chem Phys* 2001, 202, 1631.
2. Yang, J.; Liu, S.; Guo, X.; Luan, Y.; Su, W.; Liu, J. *Polym J* 2001, 33, 821.
3. Mo, Z.; Meng, Q.; Feng, J.; Zhang, H.; Chen, D. *Polym Int* 1993, 32, 53.
4. Zhang, H.; Yang, B.; Zhang, L.; Mo, Z. *Acta Polym Sin* 1996, 1, 1.
5. Pathmanathan, K.; Cavaille, J.-Y.; Johari, G. P. *J Polym Sci Part B: Polym Phys* 1992, 30, 341.
6. Neagu, R. M.; Neagu, E.; Kyritsis, A.; Pissis, P. *J Phys D: Appl Phys* 2000, 33, 1921.
7. Boyd, R. H. *J Chem Phys* 1959, 30, 1276.
8. McCall, D. W.; Anderson, E. W. *J Chem Phys* 1960, 32, 237.
9. Steeman, P. A. M.; Maurer, F. H. J. *Polymer* 1992, 33, 4236.
10. Pathmanathan, K.; Johari, G. P. *J Polym Sci Part B: Polym Phys* 1993, 31, 265.
11. Ahmad, M. M.; Yamada, K.; Okuda, T. *Solid State Commun* 2002, 123, 185.
12. Liu, J.; Duan, C.-G.; Yin, W.-G.; Mei, W. N.; Smith, R. W.; Hardy, J. R. *J Chem Phys* 2003, 119, 2812.
13. Neagu, E.; Pissis, P.; Apekis, L. *J Appl Phys* 2000, 87, 2914.
14. Mudarra, M.; Diaz-Calleja, R.; Belana, J.; Cañadas, J. C.; Diego, J. A.; Sellarès, J.; Sanchis, M. J. *Polymer* 2001, 42, 1647.

15. Calleja, R. D. *J Non-Cryst Solids* 1994, 172, 1413.
16. Starkweather, H. W.; Avakian, P. *J Polym Sci Part B: Polym Phys* 1992, 30, 637.
17. Huang, X.; Mo, Z.; Gao, H.; Wang, L.; Mu, Z.; Zhu, C. *Acta Polym Sinica* 1994, 1, 60.
18. Kyritsis, A.; Pissis, P.; Grammatika'kis, J. *J Polym Sci Part B: Polym Phys* 1995, 33, 1737.
19. Neagu, E.; Pissis, P.; Apekis, L.; Ribelles, J. L. G. *J Phys D: Appl Phys* 1997, 30, 1551.
20. Neagu, R. M.; Neagu, E.; Bonanos, N.; Pissis, P. *J Appl Phys* 2000, 88, 6669.
21. Davis, R. D.; Bur, A. J.; McBrearty, M.; Lee, Y.-H.; Gilman, J. W.; Start, P. R. *Polymer* 2004, 45, 6487.
22. Korzhenko, A.; Tabellout, M.; Emery, J. R. *Polymer* 1999, 40, 7187.
23. Corezzi, S.; Capaccioli, S.; Gallone, G.; Livi, A.; Rolla, P. A. *J Phys: Condens Matter* 1997, 9, 6199.
24. Stickel, F.; Fischer, E. W.; Richert, R. *J Chem Phys* 1995, 102, 6251.